Chemical Science

RSC Publishing

EDGE ARTICLE

View Article Online
View Journal | View Issue

# Photoelectron spectroscopy of solvated electrons in alcohol and acetonitrile microjets

Cite this: *Chem. Sci.*, 2013, **4**, 1633

Alexander T. Shreve,[ab] Madeline H. Elkins[a] and Daniel M. Neumark*[ab]

Photoelectron spectra of solvated electrons in methanol, ethanol, and acetonitrile microjets are reported. Solvated electrons are generated in and detached from microjets using two photons from single nanosecond laser pulses at wavelengths ranging 266 to 213 nm. We find vertical binding energies of 3.38 ± 0.11 eV in methanol and 3.38 ± 0.10 eV in ethanol. Two features are observed in acetonitrile at 2.61 ± 0.11 eV and 3.67 ± 0.15 eV, attributed to the solvated and dimer-bound binding geometries respectively. These results are compared to previous work on solvated cluster anions and alkali-doped solvent clusters.

Received 23rd November 2012
Accepted 31st January 2013

DOI: 10.1039/c3sc22063j

www.rsc.org/chemicalscience



## Introduction

Solvated electrons, $e^-_{solv}$, are among the most intriguing systems in the physical sciences, playing an important role in DNA damage,[1] radiation chemistry,[2] atmospheric aerosol chemistry,[3] and in theoretical studies as the simplest quantum mechanical solute.[4] Consequently, many experimental and theoretical methods have been used to study the chemistry, spectroscopy, and dynamics of solvated electrons.[5] However, only recently has it become possible to directly measure the vertical binding energies (VBEs) of solvated electrons in bulk solution, *via* photoelectron spectroscopy of the liquid microjet sources developed by Faubel and co-workers.[6] As illustrated in Table 1, several such experiments have been performed on $e^-_{solv}$ in water,[7] as well as methanol and ethanol.[8] It is of considerable interest to compare these results to VBEs measured for gas phase solvated electron clusters $S_n^-$ in order to test how or if the cluster VBEs extrapolate to the bulk values as $n \rightarrow \infty$.[9] While the VBEs of solvated electrons in water jets are in general agreement with extrapolated values from VBEs of water cluster anions,[10] recent work by Suzuki *et al.*[8b] finds that the VBE reported for electrons in methanol jets is 0.65 eV higher than the extrapolated value obtained from photoelectron (PE) spectra $(MeOH)_n^-$ cluster anions[11] (see Table 1). Experiments on alkali-doped solvent clusters[12] provide an additional point of comparison. With these considerations in mind, we have re-investigated the PE spectra of electrons in liquid jets of methanol (MeOH), ethanol (EtOH), and report first results for electrons in acetonitrile (MeCN).

Methanol and ethanol are very natural solvents in which to study electron solvation. As is the case with water, both alcohols have significant hydrogen-bonding networks that are disrupted to accommodate the excess electron.[13] Time-resolved studies of electron solvation in these solvents have been carried out in several laboratories.[14] Electron spin resonance (ESR) and resonance Raman (RR) spectroscopy have shown that the ground state cavity for $e^-_{solv}$ in these solvents is similar to that in water, but with only four molecules in the first solvation shell rather than the six in the case of water.[15] This bulk solvent work is complemented by PE spectroscopy of $(MeOH)_n^-$ clusters as large as $n = 460$.[11] These spectra show evidence for two distinct isomers of the cluster anions, in which isomer I, the higher binding energy species, appears to be internally solvated.[11,16] In related work, photoionization measurements on $Na(MeOH)_n$ and $Na(EtOH)_n$ clusters yield extrapolated ionization potentials (IPs) which are close to, but below the solvated electron VBEs from liquid jet experiments as shown in Table 1.[8b,12c,17]

**Table 1** Literature values of bulk excess electron binding energies

| Solvent | Anion cluster extrapolation[a] (eV) | Alkali-doped cluster extrapolation[b] (eV) | Directly measured in liquid jets[c] (eV) |
|---|---|---|---|
| Water | 3.59 | 3.17 | 3.3–3.6 |
| Methanol | 2.54 | 3.19 | 3.36–3.38 |
| Ethanol | — | 3.07 | 3.28–3.38 |
| Acetonitrile (cavity-solvated) | 1.48 | 2.4 | 2.61 |
| Acetonitrile (dimer-bound) | 3.66 | | 3.67 |

[a] Bulk binding energy extrapolations of candidate internally solvated isomers observed in anionic solvent clusters, $S_n^-$.[11,19] [b] Bulk adiabatic ionization potentials based on the extrapolation of alkali-doped neutral solvent clusters.[12,17] [c] Bulk vertical binding energies, measured directly with the liquid microjet technique, including the results presented in this work.[7a,7c,7d,8b]

[a]*Department of Chemistry, University of California, Berkeley, California 94720, USA*
[b]*Chemical Sciences Division, Lawrence Berkeley National Laboratory, Berkeley, California 94720, USA. E-mail: dneumark@berkeley.edu; Fax: +1 510-642-3635; Tel: +1 510-642-3502*

In contrast to water or methanol, liquid acetonitrile accommodates excess electrons in two very distinct binding configurations assigned to a solvated electron within a cavity and a dimer-bound anion species stabilized by its interaction with surrounding solvent molecules.[18] In the dimer species, two molecules orient anti-parallel, with CCN bond angles of ~130° and the excess electron localized by the interaction between antibonding CN orbitals.[20] Similarly, PE spectra of $(MeCN)_n^-$ clusters up to $n = 130$ show that two electron binding motifs are present: isomer I clusters with lower VBEs were attributed to the excess electron residing within a solvent cavity, while the higher VBE clusters (isomer II), which dominate the PE spectrum starting around $n = 13$, were assigned to the dimer-bound species.[19a,20b] Photoionization efficiency measurements on $Cs(MeCN)_n$ clusters extrapolate to a bulk ionization potential of 2.4 eV.[12b]

In light of the discrepancies in VBEs for solvated electrons in MeOH cluster anions and liquid jets, we have measured PE spectra in MeOH and EtOH jets with a somewhat different experimental configuration than that used by Suzuki. We also report the first results on excess electrons in MeCN liquid jets in order to see how the two proposed electron binding motifs in liquid phase and anion cluster experiments manifest themselves in photoelectron spectroscopy experiments.

## Experimental

We generate solvated electrons in liquid jets through charge-transfer-to-solvent (CTTS) excitation of iodide in solution with one photon,[18b,21] and then detach electrons to vacuum with a second photon. Both photons come from a single pulse from a nanosecond Nd:YAG laser, in contrast to the femtosecond pump-probe experiments carried out in other laboratories.[7a,7c,22] Schematically, the overall process is:

$$I^-_{(solv)} \xrightarrow{h\nu_1} I^{-*}_{(solv)} \xrightarrow{CTTS} I_{(solv)} + e^-_{(solv)} \xrightarrow{h\nu_2} I_{(solv)} + e^-_{(g)}\ (eKE).$$

Because this experiment is carried out with a single laser pulse, we do not control the delay between $h\upsilon_1$ and $h\upsilon_2$, but the equilibration time for electrons in these solutions is much less than the laser pulse duration.[18c,23] As such, the detached electrons should be fully solvated prior to photoejection. The experiments were conducted using methanol (Fisher, optima grade), ethanol (Fisher, absolute grade), and acetonitrile (Fisher, HPLC grade). To minimize exposure to water in the MeCN experiments, fresh bottles of dry-packed acetonitrile were used each day. Low concentrations of salt were included to provide precursor anions for the generation of solvated electrons and to minimize streaming potentials.[24] Solutions variously included potassium iodide (Fisher, ≥99.0% purity), sodium iodide (Mallinckrodt, AR), tetrabutylammonium iodide (TBAI, Aldrich, ≥99.0% purity), or tetrabutylammonium chloride (TBACl, Aldrich, ≥97.0% purity).

To test for any effects of water, an ultra-dry run of acetonitrile was conducted. For this experiment, acetonitrile was dried over activated 3 Å molecular sieves for 96 hours, resulting in an expected water content below 10 ppm,[25] while the TBAI was dried by heating under vacuum overnight. All solution vessels were dried by baking at 150 °C overnight, with the solution subsequently prepared under dry nitrogen in a glove box. The syringe pump and microjet assembly were dried by purging with 4.8 pure Argon for three hours, and ultra-dry MeCN for an hour.

Our experimental apparatus was described in detail previously.[7d] Briefly, the apparatus comprises a liquid source chamber and a time-of-flight (TOF) chamber. Bulk solutions were introduced to vacuum by applying high pressure (40–150 atm) to solution behind a 20 μm ID fused silica capillary. The resulting flow was a microjet that remained laminar for at least 1 mm, and usually for 4 mm. Flow rates of 0.250 mL $min^{-1}$ were normally used, resulting in jet velocities of 13 m $s^{-1}$. The jets were collected in a liquid nitrogen cooled trap, with the liquid jet region typically achieving pressures of $2 \times 10^{-4}$ Torr with methanol, $1 \times 10^{-4}$ with ethanol, and $2 \times 10^{-4}$ Torr with MeCN.

The jet was crossed 1 mm downstream from the nozzle with the output of a 30 Hz Nd:YAG laser, operating at 266, 247, 231, or 213 nm. Laser harmonics were produced in BBO crystals, while 247 and 231 nm pulses were produced as anti-Stokes lines of 266 nm light focused into a 65 cm long Raman cell filled with 250 psi of deuterium gas. Laser pulses were typically 8 ns long, with 0.3–1.5 μJ per pulse.

Once in vacuum, electrons were sampled by a 500 μm skimmer located 1 mm from the jet. The electrons then traveled through a 60 cm field free drift tube to a Z-stack multichannel plate detector. The resulting arrival time distributions were averaged on a digital oscilloscope, transferred to a computer, and summed, typically for $10^5$ laser shots. Raw time-of-flight spectra were then converted to eKE spectra using the appropriate Jacobian transformation ($t^{-3}$). The detector region was pumped by three turbomolecular pumps, with a combined pumping speed of 1650 L $s^{-1}$. Typical detector pressures were $4 \times 10^{-6}$ Torr with methanol, $2 \times 10^{-6}$ with ethanol, and $3 \times 10^{-6}$ Torr with MeCN.

In a significant improvement since our previous report,[7d] the spectrometer was calibrated by three-photon ionization of Xe to the $Xe^+$ $^2P_{3/2}$ and $^2P_{1/2}$ states by 150 fs laser pulses at 250 or 266 nm (4–9 μJ per pulse, 1 kHz). A Clark-MXR CPA-1000 laser system generated femtosecond pulses at 800 nm, which were either frequency-tripled to generate 266 nm light or routed into a commercial OPA (TOPAS, Light Conversion Ltd) with light at 250 nm generated from the second harmonic of the sum-frequency signal. Trigger timing differences between the two laser systems were corrected by matching the respective time origins as measured by scattered light in the flight tube.

This new scheme allowed us to calibrate while the liquid jet was running and directly measure the streaming potential of the jets. Following the methodology of Shen *et al.*,[8a] the liquid jet was moved away from the laser interaction point while the shift in the kinetic energy of the $Xe^+(^2P_{3/2})$ photoelectron peak was observed. The kinetic energy of these electrons is then given by

$$eKE(x) = eKE_{field\text{-}free} - \phi_{str}\frac{L}{(L + x)}, \quad (1)$$

where $eKE_{field\text{-}free}$ is the kinetic energy of these electrons in the absence of a field from the liquid jet, $\phi_{str}$ is the streaming

 

potential of the jet, $L$ is the (fixed) distance from the skimmer to the laser, and $x$ is the distance between the jet and laser. The field-free kinetic energy was measured each day after stopping the jet to account for day-to-day changes in the laser wavelength. The conversion of our solvated electron kinetic energy spectra to electron binding energy (eBE) is then given by

$$\mathrm{eBE} = h\nu - \mathrm{eKE} - \phi_{\mathrm{str}}, \quad (2)$$

where $h\nu$ is the photon energy.

Temperatures for each solvent were estimated using the evaporative cooling numerical simulation described by Faubel *et al.*[6a] and implemented by Smith *et al.*[26] Jets were treated as thirty concentric annular columns of equal radial width, with distinct temperatures and heat exchange between them. The temperature dependence of the vapor pressure is explicitly accounted for, while other physical properties are treated as constant at their room temperature values. Since each annulus is significantly thicker than our probe depth, our temperatures are taken to be those of the outer annulus in each calculation. We estimate the methanol jets have cooled to 250 K, the ethanol jets to 260 K, and the acetonitrile jets to 250 K.

## Results

Methanol data were recorded using 100 mM KI solutions at 213 nm, near the I($^2P_{3/2}$) peak of the CTTS band at 220 nm at 298 K.[21b] A typical photoelectron spectrum, plotted *versus* eBE and corrected for streaming potential, is presented in Fig. 1A. VBEs, taken as the center of a Gaussian fit to the spectra, are found to be 3.38 ± 0.11 eV, while the peak widths are 1.26 ± 0.11 eV full width at half maximum (FWHM). The streaming potentials for these jets were typically ~400 mV; uncorrected VBEs were ~3.8 eV. Ethanol data were collected using 200 mM NaI solutions at 231 nm, near the maximum of the iodide CTTS band at 219 nm at 298 K.[21a] A representative spectrum is shown in Fig. 1B. Typical streaming potentials for ethanol jets were ~120 mV, with uncorrected VBEs of ~3.5 eV. We find a corrected VBE of 3.38 ± 0.10 eV with a FWHM of 1.03 ± 0.10 eV.

Acetonitrile data were taken at 266, 247, 231, and 213 nm with either 50 mM KI or 200 mM TBAI. These wavelengths span a significant portion of the CTTS band, which has peaks at 247 and 210 nm at 298 K (5.02 and 5.92 eV, 0.34 and 0.49 eV FWHM respectively).[21b] Streaming potentials for acetonitrile jets were usually 0.10 eV. Typical corrected spectra from each wavelength are presented in Fig. 1C. Two features are observed: a peak with a VBE of 2.61 ± 0.11 eV (~2.7 eV uncorrected), FWHM 0.70 ± 0.08 eV, that is present at all wavelengths and a peak with a higher VBE of 3.67 ± 0.15 eV (~3.8 eV uncorrected), FWHM 1.29 ± 0.16 eV, that is present at every wavelength except 266 nm. The relative signal levels and peak ratios at each wavelength are presented in Table 2, normalized for laser power, number of shots, and salt concentration. All of these results were confirmed by repeated measurement over several days.

Acetonitrile is known to be hygroscopic, and one possible origin of the high VBE peak, which lies close to the VBE of hydrated electrons, is water contamination in the sample. Furthermore, it has been shown that water contamination of an acetonitrile sample can significantly alter hydrated electron dynamics following CTTS excitation, likely due to the influence of microscopic pools of water within bulk acetonitrile.[18c,27] To test for the effects of water, data were collected at 213 nm using extra dry solution prepared as described above; these data completely agreed with our other findings.

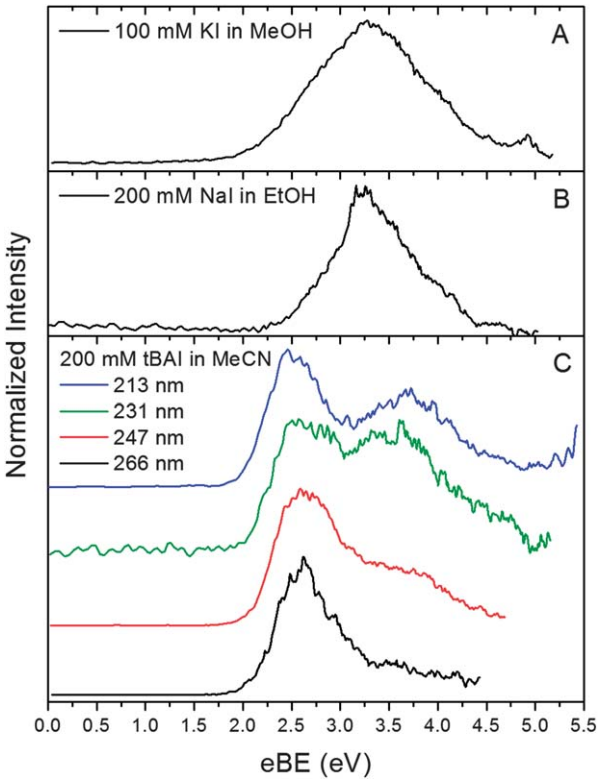


**Fig. 1** Representative spectra of electrons solvated in (A) methanol at 213 nm, (B) ethanol at 231 nm, and (C) acetonitrile at 266, 247, 231, and 213 nm. These spectra were smoothed by convolution with a 15 meV Gaussian.

**Table 2** Wavelength dependent signal level and peak ratios

| Wavelength (nm) | Relative intensity[a] | Peak ratio (low/high BE)[b] |
|---|---|---|
| 266 | 1 | — |
| 247 | 7 | 0.6 ± 0.2 |
| 231 | 2 | 0.4 ± 0.1 |
| 213 | 6 | 0.6 ± 0.2 |

[a] Total integrated signal corrected for laser power, salt concentration, and shots collected, normalized to the signal at 266 nm. [b] Ratio of integrated signals of the low and high binding energy peaks, with relative contributions determined by Gaussian two-peak fits.

## Discussion

The VBEs for $e^-_{solv}$ in both methanol and ethanol presented here are in good agreement with the findings of Horio *et al.*[8b] Our observed peak widths and streaming potentials in methanol are

larger than those reported by Horio, but agree with their findings for ethanol. The overall agreement is noteworthy because of the differences between our experiments; we generate and detach solvated electrons with two photons from the same nanosecond pulse, while Horio used two separate femtosecond pulses with a well-defined pump-probe delay. The agreement between our approaches further validates our respective approaches and underscores the importance of using a calibration obtained while the liquid jet is running. Most importantly, it shows that the VBE of solvated electrons in methanol jets is significantly higher than the extrapolated VBE from MeOH cluster anions. The general agreement between the VBE measurements in water cluster anions and water liquid jets supports the idea that it is valid to extrapolate cluster VBEs to liquid jet measurements, but the MeOH results call that conclusion into question.

In this context, the acetonitrile results are of interest as they provide an additional data point for comparing cluster and liquid jet experiments. The first point to consider is that at all excitation wavelengths except 266 nm, the liquid jet PE spectra show two peaks with VBEs of 2.61 and 3.67 eV. As described in the Results, we have made considerable effort to show that both originate from MeCN, rather than water contaminant. Since the data taken with the ultra-dry solution match our other data and the observed wavelength dependence of both peaks match the acetonitrile CTTS curve rather than that of water,[28] we believe that effort was successful. Liquid MeCN can accommodate excess electrons in two different binding motifs, cavity-solvated and dimer-bound, with the dimer-bound motif being more stable.[18] It is therefore reasonable to attribute the two peaks in the liquid jet PE spectra to these two solvation motifs, with the higher VBE feature corresponding to the dimer-bound motif. Depending on how well the cluster and liquid jet VBEs match up, such an assignment would also be consistent with the assignment of the two features in the MeCN cluster anion PE spectra where hole-burning experiments were used to verify the assignment of the tightly bound feature as the dimer-bound species.[19a]

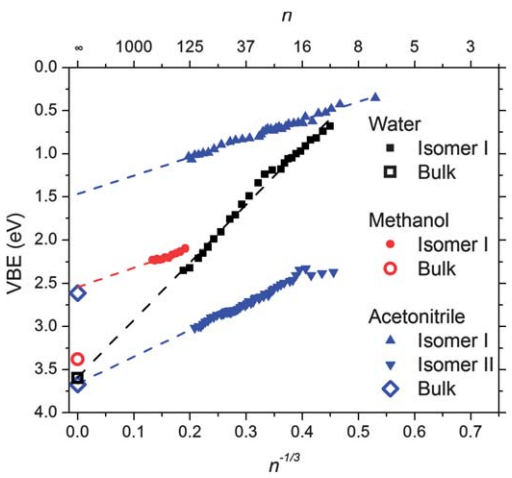


**Fig. 2** Vertical binding energy progressions for proposed internally solvated isomers of anionic water,[7d,19b] methanol,[11] and acetonitrile clusters.[19a,c]

Our findings in the bulk are compared to previous work on anionic solvent clusters $S_n^-$ in Fig. 2. This figure shows VBEs for anion clusters of water,[19b] MeOH,[11] and MeCN (ref. 19*a* and *c*) plotted *vs.* $n^{-1/3}$ and also shows VBEs obtained from liquid jet studies of the three solvents.[7d] The results for water and MeOH have been discussed above. In the case of MeCN, the VBEs for isomer II cluster anions lie on a straight line in Fig. 2 and extrapolate to 3.66 eV, very close to the VBE of 3.67 eV for the more tightly bound liquid jet feature. This correspondence supports our proposed assignment of the 3.67 eV liquid jet feature to dimer-bound solvated electrons in MeCN. The size-dependent VBEs for isomer I clusters also lie on a straight line and extrapolate to a bulk VBE of 1.48 eV, considerably less than the low VBE peak in the liquid jet spectrum.

Comparisons of the anion cluster and liquid jet VBEs with the ionization potentials of alkali-doped clusters of $H_2O$, MeOH, EtOH, and MeCN (*i.e.* $Na(H_2O)_n$, *etc.*) are also of interest. Theoretical studies of these species indicate that the electron nominally associated with the alkali atom is actually quite diffuse and exhibits some similarities to bulk solvated electrons.[12c,29] Experimental IP trends for these clusters are very different from the VBEs in bare cluster anions. For water and the two alcohols, the IPs drop upon addition of the first four waters or the first six alcohols, and then remain flat as more solvent molecules are added out to a maximum cluster size of 35–40.[12a,c,17] The extrapolated IPs for sodium-doped water, methanol, and ethanol clusters, presented in Table 1, lie close to but slightly below the corresponding liquid jet VBEs. The pattern of IPs is more complicated in $Cs(MeCN)_n$ clusters[12b] and does not flatten out until $n = 12$, where it remains constant at 2.4 eV out to $n = 21$, the largest cluster studied. This value lies close to but below the lower VBE feature, 2.61 eV, seen in MeCN liquid jets. Hence, the extrapolated IPs for all cluster types exhibit the same trend with respect to the liquid jet VBEs assigned to cavity-solvated electrons. As pointed out by Liu and Gao[29c] and Dauster *et al.*,[12c] the alkali-doped cluster experiments yield adiabatic rather than vertical IPs, consistent with the lower values relative to the liquid jet measurements. The adiabatic ionization process is believed to come about from auto-ionization following a vertical excitation of the cluster to a Rydberg state and subsequent solvent reorganization.[12c,29c] From the remarkable correspondence between the alkali-doped cluster and microjet experiments, it appears that this ionization process allows the clusters to access geometries that are representative of bulk liquid conditions despite their low temperatures.

Based on the liquid jet VBEs, the extrapolated anion cluster VBEs, and the IPs of alkali-doped solvent clusters, each liquid jet VBE can be correlated with at least one cluster measurement. However, the extrapolated VBEs for $(MeOH)_n^-$ and isomer I $(MeCN)_n^-$ clusters do not match any other measurements. In both cases, the maximum cluster size was quite large ($n = 460$ for MeOH and 130 for MeCN), so it is unlikely that this discrepancy would be resolved by going to bigger clusters. Forck *et al.*[17] have suggested that this situation arises for MeOH because the methanol cluster anions are solid rather than liquid. Their argument is based on a comparison of the slope of

 

the VBE *vs.* $n^{-1/3}$ plot with the predictions of dielectric continuum (DC) theory.[30] A similar situation may hold for isomer I acetonitrile cluster anions, too.

In DC theory, the solvated electron is treated as a spherical charge in a void, surrounded by a dielectric continuum. As such, the model is inappropriate to apply to the dimer-bound species, but it can be applied to all other cases considered here. Using DC theory, the size-dependent vertical binding energies VBE($n$) for these clusters are given by

$$\mathrm{VBE}(n) = \mathrm{VBE}(\infty) - \frac{e^2}{8\pi\varepsilon_0 r_0}\left(1 + \frac{1}{\varepsilon_\infty} - \frac{2}{\varepsilon_s}\right)n^{-1/3}, \quad (3)$$

$$\mathrm{VBE}(\infty) = \frac{e^2}{8\pi\varepsilon_0 a_0}\left(1 + \frac{1}{\varepsilon_\infty} - \frac{2}{\varepsilon_s}\right). \quad (4)$$

here VBE($\infty$) is the bulk VBE, $r_0$ is the average molecular radius, $a_0$ is the bulk cavity radius occupied by $e^-_{solv}$, $\varepsilon_0$ is the permittivity of free space, while $\varepsilon_\infty$ and $\varepsilon_s$ are respectively the solvent optical and static dielectric constants. The radius can be estimated from the bulk molar volume, while the molecular dielectric constants are taken from literature values.[31–33,35–39] Where available, the cavity radii are estimated by moment analysis of the electron absorption spectra from 0.1 eV to 6.0 eV (ref. 40) at appropriate temperatures.[17,34,37,41,42]

Table 3 presents a quantitative comparison of DC theory and experimental findings for water and the three solvents considered here. Based on the parameters for water, the slope of the cluster VBE progression predicted by DC theory for solids and liquids can be used to assign a cluster phase. The experimental slopes and extrapolated VBEs for isomer I of both $(MeOH)_n^-$ and $(MeCN)_n^-$ clusters are in better agreement with the DC theory prediction based on parameters for the solids than the liquids. The difference in predicted slopes between phases is dominated by the order of magnitude difference in the static dielectric constants, so the assignment is insensitive to small errors in any of the parameters.

It would be of considerable interest to investigate photoelectron spectra of MeOH and MeCN cluster anions as a function of temperature to see if higher VBE clusters are formed at higher temperatures. Several laboratories have incorporated ion trapping and cooling into anion photodetachment experiments,[10c,43] enabling one to vary the cluster temperature systematically and test for its effect on the photoelectron spectrum. However, if the cluster temperature is raised too high, extensive solvent evaporation can occur, along with ejection of the excess electron *via* thermionic emission, so it remains to be seen if a shift in VBE can be seen before these other effects become dominant. One would also like to understand if there is more systematic agreement between liquid jet VBEs and extrapolated IPs of alkali-doped solvent clusters than with VBEs from anion clusters. We expect these issues to be addressed in future experimental and theoretical studies on liquid jets and clusters.

## Conclusions

We have measured the photoelectron spectra of solvated electrons in methanol, ethanol, and acetonitrile. We find vertical binding energies of 3.38 ± 0.11 eV for $e^-_{solv}$ in ~250 K MeOH and 3.38 ± 0.10 eV in ~260 K EtOH. Two species of excess electrons are observed in MeCN at ~250 K, with VBEs of 2.61 ± 0.11 eV and 3.67 ± 0.15 eV. These VBEs are attributed to cavity-solvated and dimer-bound motifs, respectively. This is the first reported direct measurement of electron binding energies in acetonitrile, and our alcohol VBEs are in good agreement with the recent report of Horio *et al.*[8b]

These findings are particularly interesting in light of studies on small solvent clusters. As was observed for the bulk hydrated electron,[7] the bulk, dimer-bound excess electron in acetonitrile VBE is accurately predicted by an extrapolation of $(MeCN)_n^-$ isomer II binding energies. Unfortunately, this predictive ability is not universally true. Extrapolations of isomer I VBEs in both $(MeCN)_n^-$ and $(MeOH)_n^-$ clusters predict significantly less tightly bound electrons than are observed in the bulk. We suggest that this situation reflects the phase of the clusters, which based on DC theory, appears to be solid rather than

**Table 3** Parameters used in dielectric continuum model calculations for each solvent

| Solvent | $\varepsilon_\infty$ [a] | $\varepsilon_s$ [b] | $a_0$ [c] (Å) | $r_0$ [d] (Å) | DC slope (eV) | Exp. slope[e] (eV) | DC VBE($\infty$) (eV) | Cluster VBE($\infty$)[e] (eV) | Exp. liquid jet VBE[f] (eV) |
|---|---|---|---|---|---|---|---|---|---|
| Water (l) | 1.78 | 84.2 | 2.45 | 1.93 | −5.74 | −6.65 | 4.52 | 3.59 | 3.6 |
| Water (s) | 2.01 | 91.5 | 2.35 | 1.98 | −5.37 | | 4.52 | | |
| Methanol (l) | 1.81 | 47.4 | 2.15 | 2.48 | −4.38 | | 5.06 | | 3.38 |
| Methanol (s) | 1.74 | 3.0 | 2.5 | 2.30 | −2.84 | −2.25 | 2.61 | 2.54 | |
| Ethanol (l) | 1.86 | 30 | 2.18 | 2.81 | −3.77 | — | 4.86 | — | 3.38 |
| Acetonitrile (l) | 1.87 | 37.5 | 3.24 | 2.71 | −3.96 | | 3.31 | | 2.61 |
| Acetonitrile (s) | 1.72 | 3.8 | 3.62 | 2.52 | −3.01 | −2.14 | 2.10 | 1.48 | |

[a] Optical dielectric constants, taken as the square of the extrapolated index of refraction from ref. 31 (liquid $H_2O$, MeOH, and MeCN), ref. 32 (solid $H_2O$ and MeOH), ref. 33 (liquid EtOH), or ref. 34 (solid MeCN). [b] Static dielectric constants, with liquid water from ref. 35, solid water from ref. 36, liquid ROH from ref. 37, solid MeOH from ref. 38, and both phases of acetonitrile from ref. 39. [c] Solvated electron cavity radius, as calculated by moment analysis of the absorption spectra from 0.1 eV to 6.0 eV (ref. 40) at appropriate phases and temperatures where available. Water from ref. 41, liquid MeOH from ref. 37, solid MeOH from ref. 17, liquid EtOH from ref. 37, and liquid MeCN from ref. 42. Solid MeCN is taken by approximation such that the difference between the solvated cavity radii between phases is twice the difference in molecular radii between phases, as is the case for water and methanol. [d] Average molecular radii, taken from molar volumes using densities at room temperature or the freezing point. [e] Experimental cluster results from ref. 19*b* (water), 11 (MeOH), and ref. 19*a* and *c* (MeCN). [f] Experimental VBE as measured in liquid jets. The water value is taken from ref. 7*d* others, this work.

liquid. Intriguingly, the adiabatic IPs of alkali-doped neutral clusters extrapolate to values slightly below the bulk VBEs assigned to cavity-bound electrons in all of four solvents. Both of these cluster trends merit further investigation.

## Acknowledgements

Support for this work was provided by the National Science Foundation through Grant CHE-1011819. Thanks to Michael Lipschutz for assistance in preparation of the extra dry acetonitrile solution.



## Notes and references

1 (*a*) J. Simons, *Acc. Chem. Res.*, 2006, **39**, 772–779; (*b*) E. Alizadeh and L. Sanche, *Chem. Rev.*, 2012, **112**, 5578–5602; (*c*) J. Gu, J. Leszczynski and H. F. Schaefer, *Chem. Rev.*, 2012, **112**, 5603–5640.

2 (*a*) C. D. Jonah, D. M. Bartels and A. C. Chernovitz, *Radiat. Phys. Chem.*, 1989, **34**, 145–156; (*b*) J. Belloni, *Nukleonika*, 2011, **56**, 203–211.

3 F. Arnold, *Nature*, 1981, **294**, 732–733.

4 (*a*) P. J. Rossky and J. Schnitker, *J. Phys. Chem.*, 1988, **92**, 4277–4285; (*b*) L. Turi and P. J. Rossky, *Chem. Rev.*, 2012, **112**, 5641–5674.

5 (*a*) J. V. Coe, *Int. Rev. Phys. Chem.*, 2001, **20**, 33–58; (*b*) J. M. Herbert and L. D. Jacobson, *Int. Rev. Phys. Chem.*, 2011, **30**, 1–48; (*c*) K. R. Siefermann and B. Abel, *Angew. Chem., Int. Ed.*, 2011, **50**, 5264–5272; (*d*) B. Abel, U. Buck, A. L. Sobolewski and W. Domcke, *Phys. Chem. Chem. Phys.*, 2012, **14**, 22–34.

6 (*a*) M. Faubel, S. Schlemmer and J. P. Toennies, *Z. Phys. D*, 1988, **10**, 269–277; (*b*) M. Faubel, B. Steiner and J. P. Toennies, *J. Chem. Phys.*, 1997, **106**, 9013–9031; (*c*) B. Winter and M. Faubel, *Chem. Rev.*, 2006, **106**, 1176–1211.

7 (*a*) K. R. Siefermann, Y. X. Liu, E. Lugovoy, O. Link, M. Faubel, U. Buck, B. Winter and B. Abel, *Nat. Chem.*, 2010, **2**, 274–279; (*b*) Y. Tang, H. Shen, K. Sekiguchi, N. Kurahashi, T. Mizuno, Y.-I. Suzuki and T. Suzuki, *Phys. Chem. Chem. Phys.*, 2010, **12**, 3653–3655; (*c*) A. Lübcke, F. Buchner, N. Heine, I. V. Hertel and T. Schultz, *Phys. Chem. Chem. Phys.*, 2010, **12**, 14629–14634; (*d*) A. T. Shreve, T. A. Yen and D. M. Neumark, *Chem. Phys. Lett.*, 2010, **493**, 216–219.

8 (*a*) H. Shen, N. Kurahashi, T. Horio, K. Sekiguchi and T. Suzuki, *Chem. Lett.*, 2010, **39**, 668–670; (*b*) T. Horio, H. Shen, S. Adachi and T. Suzuki, *Chem. Phys. Lett.*, 2012, **535**, 12–16.

9 (*a*) D. M. Neumark, *Mol. Phys.*, 2008, **106**, 2183–2197; (*b*) R. M. Young and D. M. Neumark, *Chem. Rev.*, 2012, 5553–5577.

10 (*a*) J. V. Coe, G. H. Lee, J. G. Eaton, S. T. Arnold, H. W. Sarkas, K. H. Bowen, C. Ludewigt, H. Haberland and D. R. Worsnop, *J. Chem. Phys.*, 1990, **92**, 3980–3982; (*b*) J. R. R. Verlet, A. E. Bragg, A. Kammrath, O. Cheshnovsky and D. M. Neumark, *Science*, 2005, **307**, 93–96; (*c*) L. Ma, K. Majer, F. Chirot and B. von Issendorff, *J. Chem. Phys.*, 2009, **131**, 144303–144306; (*d*) G. B. Griffin, R. M. Young, O. T. Ehrler and D. M. Neumark, *J. Chem. Phys.*, 2009, **131**, 194302–194309.

11 A. Kammrath, J. R. R. Verlet, G. B. Griffin and D. M. Neumark, *J. Chem. Phys.*, 2006, **125**, 171102.

12 (*a*) I. V. Hertel, C. Hüglin, C. Nitsch and C. P. Schulz, *Phys. Rev. Lett.*, 1991, **67**, 1767–1770; (*b*) F. Misaizu, K. Tsukamoto, M. Sanekata and K. Fuke, *Chem. Phys. Lett.*, 1992, **188**, 241–246; (*c*) I. Dauster, M. A. Suhm, U. Buck and T. Zeuch, *Phys. Chem. Chem. Phys.*, 2008, **10**, 83–95.

13 K. R. Wilson, M. Cavalleri, B. S. Rude, R. D. Schaller, T. Catalano, A. Nilsson, R. J. Saykally and L. G. M. Pettersson, *J. Phys. Chem. B*, 2005, **109**, 10194–10203.

14 (*a*) X. Shi, F. H. Long, H. Lu and K. B. Eisenthal, *J. Phys. Chem.*, 1995, **99**, 6917–6922; (*b*) C. Silva, P. K. Walhout, P. J. Reid and P. F. Barbara, *J. Phys. Chem. A*, 1998, **102**, 5701–5707; (*c*) A. Thaller, R. Laenen and A. Laubereau, *J. Chem. Phys.*, 2006, 124; (*d*) X. Y. Chen and S. E. Bradforth, *Annu. Rev. Phys. Chem.*, 2008, **59**, 203–231.

15 (*a*) L. Kevan, *Chem. Phys. Lett.*, 1979, **66**, 578–580; (*b*) M. Narayana and L. Kevan, *J. Am. Chem. Soc.*, 1981, **103**, 1618–1622; (*c*) C. M. Stuart, M. J. Tauber and R. A. Mathies, *J. Phys. Chem. A*, 2007, **111**, 8390–8400.

16 L. Mones, P. J. Rossky and L. Turi, *J. Chem. Phys.*, 2011, **135**, 084501.

17 R. M. Forck, I. Dauster, U. Buck and T. Zeuch, *J. Phys. Chem. A*, 2011, **115**, 6068–6076.

18 (*a*) I. A. Shkrob and M. C. Sauer, *J. Phys. Chem. A*, 2002, **106**, 9120–9131; (*b*) C. Xia, J. Peon and B. Kohler, *J. Chem. Phys.*, 2002, **117**, 8855–8866; (*c*) S. C. Doan and B. J. Schwartz, *J. Phys. Chem. B*, 2012, DOI: 10.1021/jp303591h.

19 (*a*) M. Mitsui, N. Ando, S. Kokubo, A. Nakajima and K. Kaya, *Phys. Rev. Lett.*, 2003, **91**, 153002; (*b*) A. Kammrath, J. R. R. Verlet, G. B. Griffin and D. M. Neumark, *J. Chem. Phys.*, 2006, **125**, 076101; (*c*) A. Nakajima, private communication.

20 (*a*) I. A. Shkrob, K. Takeda and F. Williams, *J. Phys. Chem. A*, 2002, **106**, 9132–9144; (*b*) T. Takayanagi, T. Hoshino and K. Takahashi, *Chem. Phys.*, 2006, **324**, 679–688.

21 (*a*) M. F. Fox and E. Hayon, *J. Chem. Soc., Faraday Trans. 1*, 1976, **72**, 1990–1996; (*b*) M. F. Fox and E. Hayon, *J. Chem. Soc., Faraday Trans. 1*, 1977, **73**, 1003–1016.

22 T. Suzuki, *Int. Rev. Phys. Chem.*, 2012, **31**, 265–318.

23 W. J. Chase and J. W. Hunt, *J. Phys. Chem.*, 1975, **79**, 2835–2845.

24 M. Faubel and B. Steiner, *Ber. Bunsen-Ges. Phys. Chem.*, 1992, **96**, 1167–1172.

25 D. B. G. Williams and M. Lawton, *J. Org. Chem.*, 2010, **75**, 8351–8354.

26 J. D. Smith, C. D. Cappa, W. S. Drisdell, R. C. Cohen and R. J. Saykally, *J. Am. Chem. Soc.*, 2006, **128**, 12892–12898.

27 (*a*) K. L. Rowlen and J. M. Harris, *Anal. Chem.*, 1991, **63**, 964–969; (*b*) J. E. Bertie and Z. Lan, *J. Phys. Chem. B*, 1997, **101**, 4111–4119; (*c*) A. E. Bragg, G. U. Kanu and B. J. Schwartz, *J. Phys. Chem. Lett.*, 2011, **2**, 2797–2804.

28 M. C. R. Symons and S. E. Jackson, *J. Chem. Soc., Faraday Trans. 1*, 1979, **75**, 1919–1928.

 

29 (*a*) R. N. Barnett and U. Landman, *Phys. Rev. Lett.*, 1993, **70**, 1775–1778; (*b*) K. Hashimoto and K. Morokuma, *J. Am. Chem. Soc.*, 1994, **116**, 11436–11443; (*c*) B. Gao and Z.-F. Liu, *J. Chem. Phys.*, 2007, **126**, 084501.
30 G. Makov and A. Nitzan, *J. Phys. Chem.*, 1994, **98**, 3459–3466.
31 G. Openhaim and E. Grushka, *J. Chromatogr., A*, 2002, **942**, 63–71.
32 W. Viehmann and A. G. Eubanks, *Effects of Surface Contamination on the Infrared Emissivity and Visible-Light Scattering of Highly Reflective Surfaces at Cryogenic Temperatures*, Report TN D-6585, NASA, Washington D.C., 1972.
33 R. Jiménez Riobóo, M. Philipp, M. Ramos and J. Krüger, *Eur. Phys. J. E*, 2009, **30**, 19–26.
34 H. M. Marla, F. F. Robert, W. J. Moore and H. Reggie, *Astrophys. J., Suppl. Ser.*, 2010, **191**, 96–112.
35 N. E. Hill, *J. Phys. Chem.*, 1970, **3**, 238–239.
36 R. P. Auty and R. H. Cole, *J. Chem. Phys.*, 1952, **20**, 1309–1314.
37 K. N. Jha, G. L. Bolton and G. R. Freeman, *J. Phys. Chem.*, 1972, **76**, 3876–3883.
38 D. W. Davidson, *Can. J. Chem.*, 1957, **35**, 458–473.
39 A. Wurflinger, *Ber. Bunsen-Ges. Phys. Chem.*, 1980, **84**, 653–657.
40 D. M. Bartels, *J. Chem. Phys.*, 2001, **115**, 4404–4405.
41 Y. Du, E. Price and D. M. Bartels, *Chem. Phys. Lett.*, 2007, **438**, 234–237.
42 I. P. Bell, M. A. J. Rodgers and H. D. Burrows, *J. Chem. Soc., Faraday Trans. 1*, 1977, **73**, 315–326.
43 (*a*) X. B. Wang and L. S. Wang, *Rev. Sci. Instrum.*, 2008, **79**, 073108; (*b*) C. Hock, J. Kim, M. Weichman, T. I. Yacovitch and D. M. Neumark, *J. Chem. Phys.*, 2012, **137**, 224201.